

Exciton-Polariton hybrid skin-topological states

Ruiqi Bao^{1,2,*}, R. Banerjee¹, S. Mandal³, Huawen Xu⁴, Shiji Li², Junfeng Gao^{2,†} and Timothy C. H. Liew^{1‡}

¹*Division of Physics and Applied Physics, School of Physical and Mathematical Sciences, Nanyang Technological University, Singapore 637371, Singapore*

²*Laboratory of Materials Modification by Laser, Ion and Electron Beams, Ministry of Education, Dalian University of Technology, Dalian, 116024 China*

³*Department of Physics, Indian Institute of Technology Bombay, Mumbai 400076, India*

⁴*Beijing Academy of Quantum Information Sciences, Beijing 100193, China*

The non-Hermitian skin effect (NHSE), where bulk states accumulate at system boundaries, challenges the conventional bulk-boundary correspondence. Here we propose a scheme to realize hybrid skintopological states (HSTS) in exciton polariton honeycomb lattices by introducing sublattice-dependent gain and loss. This non-Hermiticity couples with the intrinsic topological edge modes, leading to relocation of edge states. We show two distinct regimes: hybrid skinChern states with switchable localization controlled by TETM splitting (characterized by a change in spectral winding number from $w = 2$ to $w = -1$), and hybrid skinantichiral states which preserves the spin-polarized property. Our results bridge polariton spin physics and non-Hermitian topology, opening routes toward controllable non-reciprocal and spin-polarized transport.

Introduction. Non-Hermitian Hamiltonians are used to describe open quantum systems especially those having dissipation and gain. Non-Hermitian systems have attracted intense research interest in recent years, particularly due to their ability to host new topological phases that have no counterparts in Hermitian systems [1–4]. Among them, the non-Hermitian skin effect (NHSE), where bulk states accumulate at the edge of a finite system, violates the conventional bulk-boundary correspondence (BBC) in Hermitian topological cases [5–12] and stimulates research across photonics [13], acoustics, and electronic platforms [14–23].

Building upon these advancements, recent research has turned to explore the effects of the NHSE on topologically protected states, aiming to understand the interplay between topology and non-Hermiticity. The interplay between the NHSE and one-dimensional topological states or defect states has shown its ability to manipulate the spatial distribution of states which is called non-Hermitian morphing [24, 25]. In Chern insulators, the coexistence of chiral edge states and the NHSE gives rise to hybrid skin-topological states (HSTS), where chiral edge modes become spatially localized even though the Chern number remains non-trivial [26–31]. Despite these advances, HSTS have thus far been explored primarily in low-frequency systems such as acoustics, electrical circuits, and microwaves [32–35]. It is essential to investigate such phenomena at optical frequencies, where strong lightmatter interactions can enable functional device architectures at the nano- to microscale. Furthermore, the influence of non-Hermiticity on antichiral edge states and on internal degrees of freedom such as optical spin remains largely unexplored, offering additional avenues for realizing novel non-Hermitian optical devices.

Exciton-polaritons, hybrid light-matter quasiparticles formed in the strong coupling regime between cavity photons and excitons [36–38], provide an ideal platform to explore these effects. Because of the exciton part, polaritons can react to external magnetic field, which leads to Zeeman splitting and breaks the time reversal (TR) symmetry. Further combined with transverse electric-transverse magnetic (TE-TM) splitting from the photon part, polaritons are known to host Chern insulators and antichiral edge states [39–43]. Polaritons are driven-dissipative systems, which means that their gain can be controlled by external non-resonant pumps. The gain/loss control makes polaritons a great platform to study non-Hermitian physics such as exceptional points [44–48], parity-time (PT) symmetry [49, 50] and also the NHSE [25, 51–54]. Although several theoretical proposals have been proposed to realize the NHSE in polariton system, they mostly rely on spin-dependent losses that are experimentally challenging to maintain due to spin relaxation in the exciton reservoir [55].

In this work, instead of relying on spin, we theoretically propose a way to realize the NHSE by considering sublattice dependent decay rates. We demonstrate two distinct types of HSTS: hybrid skin-Chern edge states (HSCS) and hybrid skin-antichiral edge states (HSAS). First, we demonstrate HSCS are relocated due to the NHSE and exhibit switchable localization characterized by spectral winding numbers. By tuning the strength of the TE-TM splitting, we drive a topological phase transition in the underlying Hermitian system (from Chern number $C = 2$ to $C = 1$), and reverse the localization direction of the HSCS. The switchable localization offers a novel mechanism for reconfiguring topological states. Second, we reveal the spin-polarized HSAS. These states are localized towards opposite directions due to the NHSE, and they inherit their spin-polarized property from their parent antichiral edge states. This results in a robust spatial separation of spin-up and spin-down channels, which is confirmed by the non-trivial spectral winding numbers.

* Corresponding author: ruiqi002@e.ntu.edu.sg

† Corresponding author: gaojf@dlut.edu.cn

‡ Corresponding author: timothyliew@ntu.edu.sg

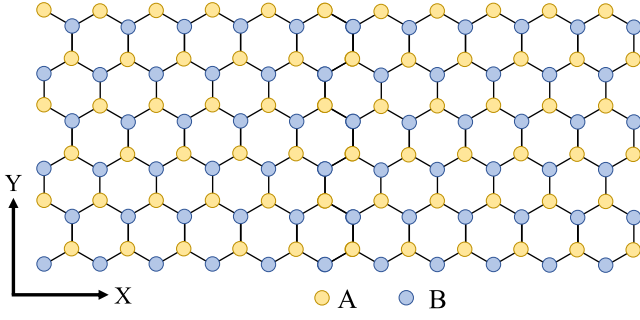


FIG. 1. Schematic figure of the non-Hermitian honeycomb lattice formed by two types of sublattices shown in yellow and blue colors separately. To make the system non-Hermitian, we set sublattice-dependent gain/loss.

Our work provides a way to create and control distinct HSTS, which is vital for non-reciprocal photonic transport and topological lasing.

Model. We start by considering a honeycomb lattice formed by two sublattices A and B in the presence of Zeeman splitting and TE-TM splitting as shown in Fig. 1. In this work, we investigate how the non-Hermitian gain/loss will influence the behaviour of the two kinds of topological states.

Polaritons correspond to a natural driven-dissipative system and in principle the loss should be the same on different sublattices (say $-i\gamma_0$). However the loss can be compensated by applying a non-resonant (effectively incoherent) pump, which serves as gain (say $iP_{A,B}$). By applying different strengths of incoherent pumps on different sublattices, the system becomes non-Hermitian ($-i\gamma_{A,B} = iP_{A,B} - i\gamma_0$). Taking periodic boundary conditions on both directions, the corresponding Hamiltonian in reciprocal space can be written in the basis of $\Psi = [\Psi_A^+, \Psi_A^-, \Psi_B^+, \Psi_B^-]^T$ as:

$$\mathcal{H}_{\mathbf{k}} = \begin{bmatrix} \Delta_A - i\gamma_A & 0 & -g_{\mathbf{k}}J & -g_{\mathbf{k}}^+ \Delta_T \\ 0 & -\Delta_A - i\gamma_A & -g_{\mathbf{k}}^- \Delta_T & -g_{\mathbf{k}}J \\ -g_{\mathbf{k}}^* J & -g_{\mathbf{k}}^* \Delta_T & \Delta_B - i\gamma_B & 0 \\ -g_{\mathbf{k}}^{+*} \Delta_T & -g_{\mathbf{k}}^* J & 0 & -\Delta_B - i\gamma_B \end{bmatrix}, \quad (1)$$

where $g_{\mathbf{k}} = \sum_{n=1}^3 \exp(-i\mathbf{k} \cdot \mathbf{r}_n)$ and $g_{\mathbf{k}}^{\pm} = \sum_{n=1}^3 \exp(-i[\mathbf{k} \cdot \mathbf{r}_n \mp 2\theta_n])$. Here \mathbf{r}_n represent the vectors connecting the three nearest "B" sites from a single "A" site (Fig. 1) and $\theta_n = 2\pi(n-1)/3$ are the angles of those vectors with respect to one of them (say \mathbf{r}_1). In the Hamiltonian, J is the coupling between the nearest neighbouring pillars, Δ_T is the TE-TM splitting, $\Delta_{A(B)}$ is the onsite energy introduced by Zeeman splitting on respective sites, $\gamma_{A(B)}$ is the effective loss on A(B) sites. Here if $\Delta_A = \Delta_B$, the system supports polariton Chern insulators, while when $\Delta_A = -\Delta_B$ the system gives polariton antichiral edge states [43].

Next, we calculate the band structures for the polari-

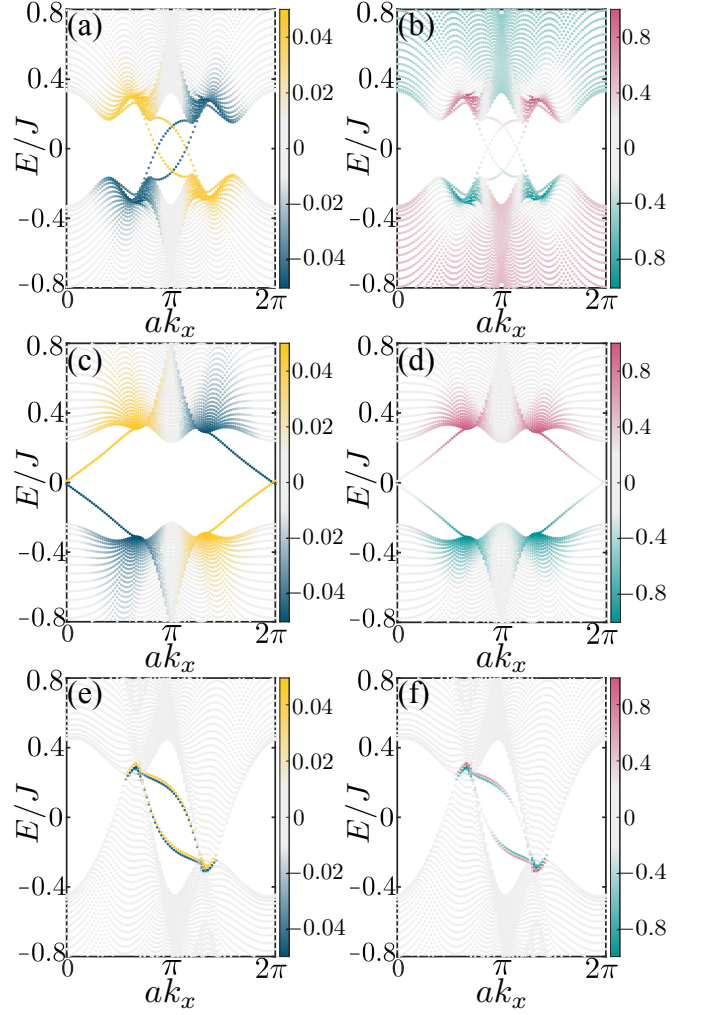


FIG. 2. Band structures for Chern insulator $C = 2$ (a-b), $C = 1$ (c-d) and antichiral edge states (e-f) in non-Hermitian regime. In (a, c, e), the states are color coded according to the imaginary term (gain/loss) and in (b, d, f) are color coded according to the DOCP. In the Chern insulator, the left propagating states and the right propagating states have different signs of imaginary energies and the states are not spin-polarized. For the antichiral case, the edge states are propagating along the same direction and still remain with the spin-polarized properties in the presence of non-Hermiticity. Parameters: $J = 1, z = 0.3J, \gamma_A = -0.05J, \gamma_B = -\gamma_A$. $\delta J = 0.3J$ for (a, b, e, f) and $\delta J = 0.6J$ for (c, d).

ton Chern insulator and the antichiral edge states in non-Hermitian regime by taking x -periodic boundary condition (PBC)/ y -open boundary condition (OBC). To better visualize the properties of topological states, here we color code the band structures according to the imaginary energies (Fig. 2(a,c,e)) and degree of circular polarization (DOCP)(Fig. 2(b,d,f)), which is defined as:

$$S_z = \frac{\sum |\Psi_{A,B}^+|^2 - \sum |\Psi_{A,B}^-|^2}{\sum |\Psi_{A,B}^+|^2 + \sum |\Psi_{A,B}^-|^2}. \quad (2)$$

In Fig. 2(a,b), the band structures for non-Hermitian Chern insulator edge states are shown ($C = 2$ case). We find that there are two pairs of edge states existed in the bandgap, consistent with the Chern number. For states with different directions of propagation, they also have different imaginary energies. The DOCP of non-Hermitian topological Chern insulators shows that the edge states are mixed spins and also bulk states are not linearly polarized.

Fig. 2(c,d) show the band structures for the case $C = 1$ obtained by changing the TE-TM splitting to $\Delta_T = 0.6J$. Only one pair of edge states remains in the band gap, again with opposite imaginary energy having opposite propagation directions. The DOCP distribution in Fig. 2(d) confirms that these states still exhibit mixed-spin character.

For the antichiral case, the edge states co-exist in the same energy range as the bulk modes and have the same direction of propagation [56]. We notice that states from different edges have different imaginary parts. The upper edge is positive and the lower edge is negative. More interestingly, we find that the edge states remain circularly polarized and states from the two opposite edges have opposite circular polarization.

We also calculate the band structures in a continuous model. The results show the change in the number of edge states in the Chern case and spin-polarized property in the antichiral case, which is consistent with our tight binding results (see Supplementary Material [57]).

Switchable hybrid skin-Chern edge states. With insights into the impact of the introduced non-Hermiticity on the band structures, we now explore its influence on the spatial localization of topological edge states. We start from the $C = 2$ case, by considering OBCs on both directions and calculate the spatial distributions of Hermitian Chern edge states. As shown in Fig. 3(a), the edge states are localized all around the boundaries of considered system in the Hermitian case. Upon applying the non-Hermitian condition, the edge states are relocalized towards left boundary (Fig. 3(b)). The redistribution of edge states suggests the appearance of hybrid skin-Chern edge states.

To verify, we calculate the energy spectrum from x -PBC/ y -OBC (black points) and both OBCs. We color coded the spectrum by the intensity weighted position (equivalent to the expectation value), which is defined as:

$$\langle x \rangle = \left(\sum_{x=1}^{N_x} x \cdot |\psi_n(x)|^2 \right) / N_x, \quad (3)$$

N_x is the number of sites along the x direction. The expectation values of position approach $1/N_x$ when eigenstates are localized at the left end; and approach 1 when they are localized at the right end. We find that the energy spectrum changes drastically when the boundary conditions are changed (Fig. 3(c)) and the energies of topological edge states from both OBCs are surrounded

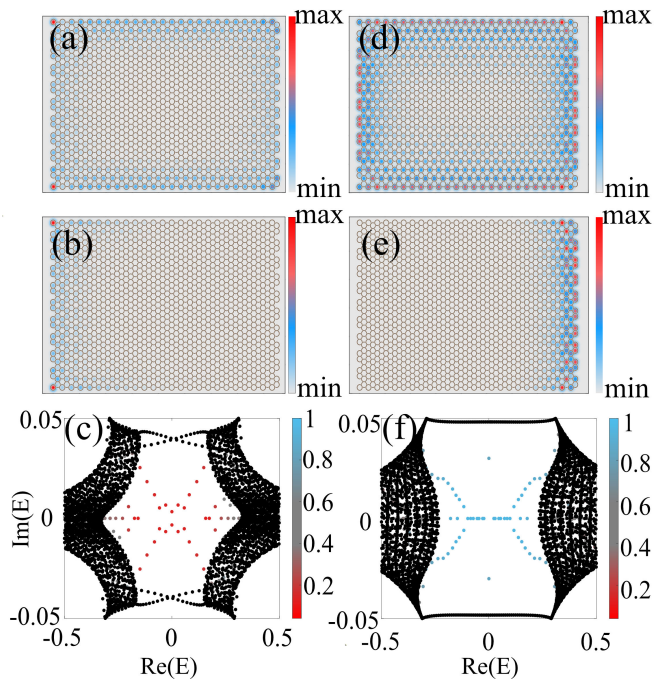


FIG. 3. (a,d) Spatial distribution of Hermitian Chern edge states. (b,e) Spatial distribution of the HSCS in two cases. The localization direction can be switched (c,f) Energy spectrum of considered HSCS system for Chern edge states ($C = 2, C = 1$) separately under both OBCs (color coded according to the expected position) and x -PBC/ y -OBC (black points). Parameters are set the same as in Fig. 2.

by the energies from x -PBC/ y -OBC, which suggests the emergence of the NHSE on the edge states. The interplay between NHSE and the Chern edge states leads to the relocation of topological edge states and forms the HSCS. It should be noted that at the same time the bulk states are not localized. The number of HSCS does not scale as $\mathcal{O}(N_x N_y)$; instead it scales as $\mathcal{O}(N_x)$, consistent with previous works [26–31].

The direction of this NHSE-induced localization is explained by the topological invariant (winding number):

$$w = \frac{1}{2\pi i} \int_{BZ} \log \left(\frac{d}{dk} [H(k) - E_{ref}] dk \right). \quad (4)$$

In this case, our calculation yields a winding number of $w = 2$. This non-zero integer value provides direct proof of the NHSE and is consistent with the localization of the HSCS to the left boundary.

Remarkably, the localization of these HSCS is switchable. In the Hermitian case, the system undergoes a topological phase transition by tuning the TE-TM splitting (Δ_T). The Chern number changes from 2 to 1 when $\Delta_T > J/2$. The edge states of the Hermitian case are still localized all around the boundaries as shown in Fig. 3(b). Introducing the same non-Hermitian terms now shows a completely different result. The HSCS become localized at the right boundary of the system, as shown in Fig.

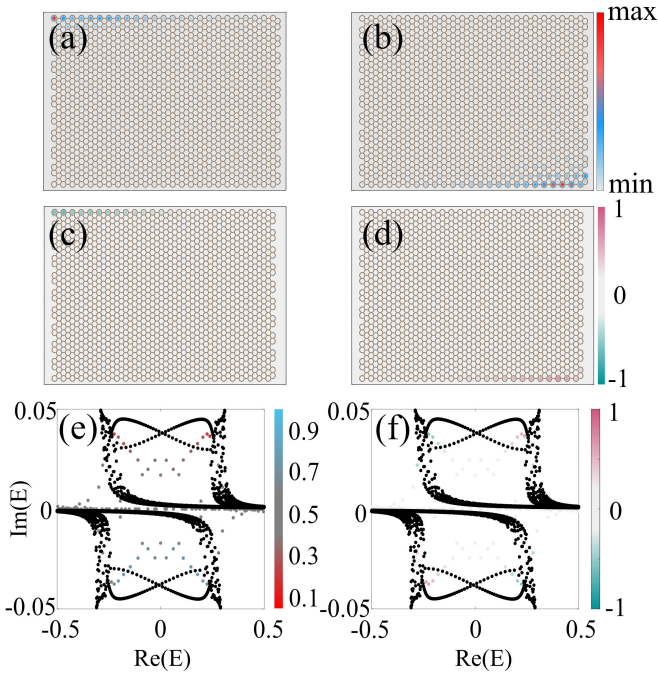


FIG. 4. (a,b) Spatial distribution of HSAS, where they are now localized towards left (a) or right (b). (c-d) DOCP of HSAS; upper edge is spin "-" and lower edge is spin "+". (e) Energy spectrum of the considered HSAS system under both OBCs (color coded according to the expected position) and x -PBC/ y -OBC (black points). (f) Energies from both OBCs are color coded according to the DOCP.

3(d). The reversal of localization can be understood by calculating the winding number which is -1 in this case. The change in the sign of the winding number directly corresponds to the direction switching of the HSCS localization from the left to the right boundary. This demonstrates a powerful method for reconfiguring topological states, where a tunable parameter can switch not only the underlying Hermitian topology but also localization behaviour of the HSCS. The switchable localization of HSCS is also demonstrated in the continuous model (see Supplementary Material [57]).

Spin-polarized hybrid skin-antichiral edge states. Having established the behaviour of the HSCS, we now turn to the antichiral edge state phase. In the Hermitian case, the edge states are localized at the upper and lower edges. When the sublattice-dependent non-Hermiticity is introduced, we find that the spatial distribution of edge states experiences drastic changes due to the NHSE and hybrid skin-antichiral edge states (HSAS) are formed. Now the states from the upper edge are localized towards the left (Fig. 4(a)), and states from lower edge are localized differently (Fig. 4(b)).

The topological origin of this phenomenon is suggested by the energy spectrum calculated from both boundary conditions (Fig. 4(e,f)) where topological states' energies from both OBCs are surrounded by x -PBC/ y -OBC. It is further confirmed by the calculation of the winding

number, which is -2 for the upper edge and 2 for the lower edge (see detailed calculation in [57]). These non-trivial topological invariants provide proof of the NHSE and explain why the two edge channels localize towards different directions of the system. This is consistent with the $\langle x \rangle$ results shown in Fig. 4(e). The edge states with $\text{Im}(E) > 0$ are localized at top-left corner (red color coded); while the edge states with $\text{Im}(E) < 0$ are localized at the bottom-right corner (blue color coded).

Furthermore, the localized HSAS inherit the spin-polarized properties from the parent Hermitian edge states. By calculating the DOCP, we reveal the intrinsic spin properties: as shown in Fig. 4(c-d), states localized at the top-left corner are spin-down polarized; while the state at the other corner is spin-up polarized. This is also consistent with the previous band structure calculations. The emergent spin separation HSAS provides a link between non-Hermitian physics and spintronic polaritonics. The spatial distribution and spin properties in a corresponding continuous model agrees well with the tight binding results (see Supplementary Material [57]).

Finally, it is essential to distinguish the corner-localized HSAS from other corner states. They are different from non-Hermitian corner states arising from higher-order skin effects, where all bulk states localize at corners and scale with the system size $\mathcal{O}(N_x N_y)$ [15, 58]. They are also distinct from Hermitian higher-order topological corner states, whose number is independent of system size ($\mathcal{O}(1)$) [59–66]. In contrast, the number of HSAS scales with $\mathcal{O}(N_x)$.

Discussion. In this work, we have theoretically proposed and analyzed the emergence of HSTS in exciton polariton honeycomb lattices induced by sublattice-dependent non-Hermiticity. By coupling the NHSE with the systems intrinsic topological edge states, we demonstrate that gainloss imbalance can relocate topological states without destroying their spin polarization.

In the Chern insulator regime, the HSCS exhibit switchable localization that can be reversed by tuning the TETM splitting. This controllable transition, characterized by a change in the spectral winding number from $w = 2$ to $w = -1$, provides a robust mechanism for manipulating non-reciprocal transport in driven dissipative systems.

Next, we showed the spin-polarized HSAS, which provides a link between the NHSE and spin degree of freedom. The resulting spin-up and spin-down polarized states are spatially separated, which may find application in spin-polarized lasing, non-reciprocal spin transport and measurement of spin-dependent polariton interactions. Importantly, the hybrid edge states remain robust against disorder and boundary defects (see Supplementary Material [57]).

The agreement between tight binding and continuous model calculations supports the feasibility of our proposal using current polariton microcavity technologies (see Supplementary Material [57]). These results could motivate future studies on the interplay between HSTS

and non-Hermitian nonlinear phenomena, paving the way to active control of non-Hermitian topological photonic and polaritonic devices.

Acknowledgement. The work was supported by the National Key R&D Program of China (Grants No.

2024YFA1409600 and No. 2024YFE0213500), the National Natural Science Foundation of China (Grants No. 12374253, No. 12374174, and No. 12004064), R&D project of Joint Funds of Liaoning Province (2023JH2/101800038), the Ministry of Education, Singapore (Grant No. MOE-MOET32023-0003).

-
- [1] Liang Feng, Ramy El-Ganainy, and Li Ge, “Non-hermitian photonics based on parity–time symmetry,” *Nature Photonics* **11**, 752–762 (2017).
 - [2] Daniel Leykam, Konstantin Y. Bliokh, Chunli Huang, Y. D. Chong, and Franco Nori, “Edge modes, degeneracies, and topological numbers in non-hermitian systems,” *Phys. Rev. Lett.* **118**, 040401 (2017).
 - [3] Ramy El-Ganainy, Konstantinos G. Makris, Mercedeh Khajavikhan, Ziad H. Musslimani, Stefan Rotter, and Demetrios N. Christodoulides, “Non-hermitian physics and pt symmetry,” *Nature Physics* **14**, 11–19 (2018).
 - [4] Kun Ding, Chen Fang, and Guancong Ma, “Non-hermitian topology and exceptional-point geometries,” *Nature Reviews Physics* **4**, 745–760 (2022).
 - [5] Shunyu Yao and Zhong Wang, “Edge states and topological invariants of non-hermitian systems,” *Phys. Rev. Lett.* **121**, 086803 (2018).
 - [6] Yifei Yi and Zhesen Yang, “Non-hermitian skin modes induced by on-site dissipations and chiral tunneling effect,” *Phys. Rev. Lett.* **125**, 186802 (2020).
 - [7] Nobuyuki Okuma, Kohei Kawabata, Ken Shiozaki, and Masatoshi Sato, “Topological origin of non-hermitian skin effects,” *Phys. Rev. Lett.* **124**, 086801 (2020).
 - [8] Fei Song, Shunyu Yao, and Zhong Wang, “Non-hermitian topological invariants in real space,” *Phys. Rev. Lett.* **123**, 246801 (2019).
 - [9] Flore K. Kunst, Elisabet Edvardsson, Jan Carl Budich, and Emil J. Bergholtz, “Biorthogonal bulk-boundary correspondence in non-hermitian systems,” *Phys. Rev. Lett.* **121**, 026808 (2018).
 - [10] Kazuki Yokomizo and Shuichi Murakami, “Non-bloch band theory of non-hermitian systems,” *Phys. Rev. Lett.* **123**, 066404 (2019).
 - [11] Zhesen Yang, Kai Zhang, Chen Fang, and Jiangping Hu, “Non-hermitian bulk-boundary correspondence and auxiliary generalized brillouin zone theory,” *Phys. Rev. Lett.* **125**, 226402 (2020).
 - [12] Kai Zhang, Zhesen Yang, and Chen Fang, “Correspondence between winding numbers and skin modes in non-hermitian systems,” *Phys. Rev. Lett.* **125**, 126402 (2020).
 - [13] Sebastian Weidemann, Mark Kremer, Tobias Helbig, Tobias Hofmann, Alexander Stegmaier, Martin Greiter, Ronny Thomale, and Alexander Szameit, “Topological funneling of light,” *Science* **368**, 311–314 (2020), <https://www.science.org/doi/pdf/10.1126/science.aaz8727>.
 - [14] Ananya Ghatak, Martin Brandenbourger, Jasper van Wezel, and Corentin Coulais, “Observation of non-hermitian topology and its bulk–edge correspondence in an active mechanical metamaterial,” *Proceedings of the National Academy of Sciences* **117**, 29561–29568 (2020), <https://www.pnas.org/remotexts.ntu.edu.sg/doi/pdf/10.1073/pnas.2010580117>.
 - [15] Xiujuan Zhang, Yuan Tian, Jian-Hua Jiang, Ming-Hui Lu, and Yan-Feng Chen, “Observation of higher-order non-hermitian skin effect,” *Nature Communications* **12**, 5377 (2021).
 - [16] Shuo Liu, Ruiwen Shao, Shaojie Ma, Lei Zhang, Oubo You, Haotian Wu, Yuan Jiang Xiang, Tie Jun Cui, and Shuang Zhang, “Non-hermitian skin effect in a non-hermitian electrical circuit,” *Research* **2021** (2021), 10.34133/2021/5608038, <https://spj.science.org/doi/pdf/10.34133/2021/5608038>.
 - [17] Qian Liang, Dizhou Xie, Zhaoli Dong, Haowei Li, Hang Li, Bryce Gadway, Wei Yi, and Bo Yan, “Dynamic signatures of non-hermitian skin effect and topology in ultracold atoms,” *Phys. Rev. Lett.* **129**, 070401 (2022).
 - [18] Zhen Li, Li-Wei Wang, Xulong Wang, Zhi-Kang Lin, Guancong Ma, and Jian-Hua Jiang, “Observation of dynamic non-hermitian skin effects,” *Nature Communications* **15**, 6544 (2024).
 - [19] Yun-Kai Liu, Pei-Chao Cao, Minghong Qi, Qiang-Kai-Lai Huang, Feng Gao, Yu-Gui Peng, Ying Li, and Xue-Feng Zhu, “Observation of non-hermitian skin effect in thermal diffusion,” *Science Bulletin* **69**, 1228–1236 (2024).
 - [20] Linhu Li, Ching Hua Lee, Sen Mu, and Jiangbin Gong, “Critical non-hermitian skin effect,” *Nature Communications* **11**, 5491 (2020).
 - [21] Li Zhang, Yihao Yang, Yong Ge, Yi-Jun Guan, Qiaolu Chen, Qinghui Yan, Fujia Chen, Rui Xi, Yuanzhen Li, Ding Jia, Shou-Qi Yuan, Hong-Xiang Sun, Hongsheng Chen, and Baile Zhang, “Acoustic non-hermitian skin effect from twisted winding topology,” *Nature Communications* **12**, 6297 (2021).
 - [22] Fei Song, Shunyu Yao, and Zhong Wang, “Non-hermitian skin effect and chiral damping in open quantum systems,” *Phys. Rev. Lett.* **123**, 170401 (2019).
 - [23] Linhu Li, Ching Hua Lee, and Jiangbin Gong, “Topological switch for non-hermitian skin effect in cold-atom systems with loss,” *Phys. Rev. Lett.* **124**, 250402 (2020).
 - [24] Wei Wang, Xulong Wang, and Guancong Ma, “Non-hermitian morphing of topological modes,” *Nature* **608**, 50–55 (2022).
 - [25] Ruiqi Bao, Huawen Xu, Wouter Verstraelen, and Timothy C. H. Liew, “Topological enhancement of exciton-polariton coherence with non-hermitian morphing,” *Phys. Rev. B* **108**, 235305 (2023).
 - [26] Ching Hua Lee, Linhu Li, and Jiangbin Gong, “Hybrid higher-order skin-topological modes in nonreciprocal systems,” *Phys. Rev. Lett.* **123**, 016805 (2019).
 - [27] Kohei Kawabata, Masatoshi Sato, and Ken Shiozaki, “Higher-order non-hermitian skin effect,” *Phys. Rev. B* **102**, 205118 (2020).
 - [28] Weiwei Zhu and Jiangbin Gong, “Hybrid skin-topological modes without asymmetric couplings,” *Phys. Rev. B* **106**, 035425 (2022).

- [29] Yaohua Li, Chao Liang, Chenyang Wang, Cuicui Lu, and Yong-Chun Liu, “Gain-loss-induced hybrid skin-topological effect,” *Phys. Rev. Lett.* **128**, 223903 (2022).
- [30] Weiwei Zhu and Linhu Li, “A brief review of hybrid skin-topological effect,” *Journal of Physics: Condensed Matter* **36**, 253003 (2024).
- [31] Junsong Sun, Chang-An Li, Shiping Feng, and Huaiming Guo, “Hybrid higher-order skin-topological effect in hyperbolic lattices,” *Phys. Rev. B* **108**, 075122 (2023).
- [32] Y. X. Fang, W. H. Zhu, Y. P. Lai, Y. Li, and S. Q. Wu, “Tunable hinge skin states in a hybrid skin-topological sonic crystal,” *arXiv* **2505.05928** (2025).
- [33] Deyuan Zou, Tian Chen, Wenjing He, Jiacheng Bao, Ching Hua Lee, Houjun Sun, and Xiangdong Zhang, “Observation of hybrid higher-order skin-topological effect in non-hermitian topoelectrical circuits,” *Nature Communications* **12**, 7201 (2021).
- [34] Tianshu Jiang, Chenyu Zhang, Ruo-Yang Zhang, Yingjuan Yu, Zhenfu Guan, Zeyong Wei, Zhanshan Wang, Xinbin Cheng, and C. T. Chan, “Observation of non-hermitian boundary induced hybrid skin-topological effect excited by synthetic complex frequencies,” *Nature Communications* **15**, 10863 (2024).
- [35] Gui-Geng Liu, Subhaskar Mandal, Peiheng Zhou, Xiang Xi, Rimi Banerjee, Yuan-Hang Hu, Minggui Wei, Maoren Wang, Qiang Wang, Zhen Gao, Hongsheng Chen, Yihao Yang, Yidong Chong, and Baile Zhang, “Localization of chiral edge states by the non-hermitian skin effect,” *Phys. Rev. Lett.* **132**, 113802 (2024).
- [36] Iacopo Carusotto and Cristiano Ciuti, “Quantum fluids of light,” *Rev. Mod. Phys.* **85**, 299–366 (2013).
- [37] Hui Deng, Hartmut Haug, and Yoshihisa Yamamoto, “Exciton-polariton bose-einstein condensation,” *Rev. Mod. Phys.* **82**, 1489–1537 (2010).
- [38] Alexey Kavokin, Timothy C. H. Liew, Christian Schneider, Pavlos G. Lagoudakis, Sebastian Klemmt, and Sven Hoeffling, “Polariton condensates for classical and quantum computing,” *Nature Reviews Physics* **4**, 435–451 (2022).
- [39] Charles-Edouard Baryn, Torsten Karzig, Gil Refael, and Timothy C. H. Liew, “Topological polaritons and excitons in garden-variety systems,” *Phys. Rev. B* **91**, 161413 (2015).
- [40] A. V. Nalitov, D. D. Solnyshkov, and G. Malpuech, “Polariton \mathbb{Z} topological insulator,” *Phys. Rev. Lett.* **114**, 116401 (2015).
- [41] S. Klemmt, T. H. Harder, O. A. Egorov, K. Winkler, R. Ge, M. A. Bandres, M. Emmerling, L. Worschech, T. C. H. Liew, M. Segev, C. Schneider, and S. Höffling, “Exciton-polariton topological insulator,” *Nature* **562**, 552–556 (2018).
- [42] S. Mandal, R. Ge, and T. C. H. Liew, “Antichiral edge states in an exciton polariton strip,” *Phys. Rev. B* **99**, 115423 (2019).
- [43] Ruiqi Bao, S. Mandal, Huawen Xu, Xingran Xu, R. Banerjee, and Timothy C. H. Liew, “Spin-polarized antichiral exciton-polariton edge states,” *Phys. Rev. B* **106**, 235310 (2022).
- [44] T. Gao, G. Li, E. Estrecho, T. C. H. Liew, D. Comber-Todd, A. Nalitov, M. Steger, K. West, L. Pfeiffer, D. W. Snoke, A. V. Kavokin, A. G. Truscott, and E. A. Ostrovskaya, “Chiral modes at exceptional points in exciton-polariton quantum fluids,” *Phys. Rev. Lett.* **120**, 065301 (2018).
- [45] A. Opala, M. Furman, M. Król, R. Mirek, K. Tyszka, B. Seredyński, W. Pacuski, J. Szczytko, M. Matuszewski, and B. Piętko, “Natural exceptional points in the excitation spectrum of a light-matter system,” *Optica* **10**, 1111–1117 (2023).
- [46] Amir Rahmani, Andrzej Opala, and Michał Matuszewski, “Exceptional points and phase transitions in non-hermitian nonlinear binary systems,” *Phys. Rev. B* **109**, 085311 (2024).
- [47] Jan Wingenbach, Stefan Schumacher, and Xuekai Ma, “Manipulating spectral topology and exceptional points by nonlinearity in non-hermitian polariton systems,” *Phys. Rev. Res.* **6**, 013148 (2024).
- [48] Yao Li, Xuekai Ma, Zaharias Hatzopoulos, Pavlos G. Savvidis, Stefan Schumacher, and Tingge Gao, “Switching off a microcavity polariton condensate near the exceptional point,” *ACS Photonics* **9**, 2079–2086 (2022).
- [49] Xuekai Ma, Yaroslav Y Kartashov, Tingge Gao, and Stefan Schumacher, “Controllable high-speed polariton waves in a pt-symmetric lattice,” *New Journal of Physics* **21**, 123008 (2019).
- [50] I. Jesán Velázquez-Reséndiz and Yuri G. Rubo, “Polarization dynamics of trapped polariton condensates with \mathcal{PT} symmetry,” *Phys. Rev. B* **109**, 085312 (2024).
- [51] S. Mandal, R. Banerjee, Elena A. Ostrovskaya, and T. C. H. Liew, “Nonreciprocal transport of exciton polaritons in a non-hermitian chain,” *Phys. Rev. Lett.* **125**, 123902 (2020).
- [52] Huawen Xu, Kevin Dini, Xingran Xu, Rimi Banerjee, Subhaskar Mandal, and Timothy C. H. Liew, “Nonreciprocal exciton-polariton ring lattices,” *Phys. Rev. B* **104**, 195301 (2021).
- [53] Subhaskar Mandal, Rimi Banerjee, and Timothy C. H. Liew, “From the topological spin-hall effect to the non-hermitian skin effect in an elliptical micropillar chain,” *ACS Photonics* **9**, 527–539 (2022).
- [54] Pavel Kokhanchik, Dmitry Solnyshkov, and Guillaume Malpuech, “Non-hermitian skin effect induced by rashba-dresselhaus spin-orbit coupling,” *Phys. Rev. B* **108**, L041403 (2023).
- [55] N. Carlon Zambon, P. St-Jean, M. Milićević, A. Lemaître, A. Harouri, L. Le Gratiet, O. Bleu, D. D. Solnyshkov, G. Malpuech, I. Sagnes, S. Ravets, A. Amo, and J. Bloch, “Optically controlling the emission chirality of microlasers,” *Nature Photonics* **13**, 283–288 (2019).
- [56] Here the edge states from both edges are degenerate, and for clarity we break the inversion symmetry by using a term $n\sigma_z \otimes \sigma_0$, $n = 10^{-2}J$. This added term only perturbs the degeneracy, is not actually needed for the existence of the states and can not influence their edge properties..
- [57] Please see the Supplementary Material for: Continuous model calculation of bandstructures; calculation of winding number; robustness against disorder and defects;.
- [58] Xingran Xu, Ruiqi Bao, and Timothy C. H. Liew, “Non-hermitian topological exciton-polariton corner modes,” *Phys. Rev. B* **106**, L201302 (2022).
- [59] Stefan Imhof, Christian Berger, Florian Bayer, Johannes Brehm, Laurens W. Molenkamp, Tobias Kiessling, Frank Schindler, Ching Hua Lee, Martin Greiter, Titus Neupert, and Ronny Thomale, “Topoelectrical-circuit realization of topological corner modes,” *Nature Physics* **14**, 925–929 (2018).
- [60] Marc Serra-Garcia, Valerio Peri, Roman Süssstrunk,

- Osama R. Bilal, Tom Larsen, Luis Guillermo Villanueva, and Sebastian D. Huber, “Observation of a phononic quadrupole topological insulator,” *Nature* **555**, 342–345 (2018).
- [61] Christopher W. Peterson, Wladimir A. Benalcazar, Taylor L. Hughes, and Gaurav Bahl, “A quantized microwave quadrupole insulator with topologically protected corner states,” *Nature* **555**, 346–350 (2018).
- [62] Motohiko Ezawa, “Higher-order topological insulators and semimetals on the breathing kagome and pyrochlore lattices,” *Phys. Rev. Lett.* **120**, 026801 (2018).
- [63] Haoran Xue, Yahui Yang, Fei Gao, Yidong Chong, and Baile Zhang, “Acoustic higher-order topological insulator on a kagome lattice,” *Nature Materials* **18**, 108–112 (2019).
- [64] Xiao-Dong Chen, Wei-Min Deng, Fu-Long Shi, Fu-Li Zhao, Min Chen, and Jian-Wen Dong, “Direct observation of corner states in second-order topological photonic crystal slabs,” *Phys. Rev. Lett.* **122**, 233902 (2019).
- [65] R. Banerjee, S. Mandal, and T. C. H. Liew, “Coupling between exciton-polariton corner modes through edge states,” *Phys. Rev. Lett.* **124**, 063901 (2020).
- [66] Jinqi Wu, Sanjib Ghosh, Yusong Gan, Ying Shi, Subhaskar Mandal, Handong Sun, Baile Zhang, Timothy C. H. Liew, Rui Su, and Qihua Xiong, “Higher-order topological polariton corner state lasing,” *Science Advances* **9**, eadg4322 (2023).